Space Sci Rev (2010) 157: 167–176
DOI 10.1007/s11214-010-9699-y

X-ray Reflection

A.C. Fabian · R.R. Ross

Received: 9 September 2010 / Accepted: 22 September 2010 / Published online: 3 November 2010

Abstract Material irradiated by X-rays produces backscattered radiation which is commonly known as the Reflection Spectrum. It consists of a structured continuum, due at high energies to the competition between photoelectric absorption and electron scattering enhanced at low energies by emission from the material itself, together with a complex line spectrum. We briefly review the history of X-ray reflection in astronomy and discuss various methods for computing the reflection spectrum from cold and ionized gas, illustrated with results from our own work REFLIONX. We discuss how the reflection spectrum can be used to obtain the geometry of the accretion flow, particularly the inner regions around black holes and neutron stars.

Keywords X-ray astronomy · Radiation processes

1 Introduction

Most accreting X-ray sources generate a hard power-law X-ray spectrum which, as well as coming directly to us, irradiates the accretion flow. The irradiation of the flow, and any other gas, produces backscattered radiation, fluorescence, recombination and other emissions. These constitute what is known as the reflection spectrum which is the topic of this review.

Note that this form of X-ray reflection does not obey the laws of reflection in the simple physics sense and should not be confused with the reflection which occurs, say, in X-ray optics. X-ray reflection is related to X-ray fluorescent spectroscopy, which is a common laboratory procedure used to non-invasively test and analyse the surface composition of a wide range of materials from cement to shampoo. It is also used to remotely determine the composition of planetary surfaces.

A.C. Fabian (✉)
Institute of Astronomy, Madingley Road, Cambridge CB3 0HA, UK
e-mail: acf@ast.cam.ac.uk

R.R. Ross
Physics Department, College of the Holy Cross, Worcester, MA, USA

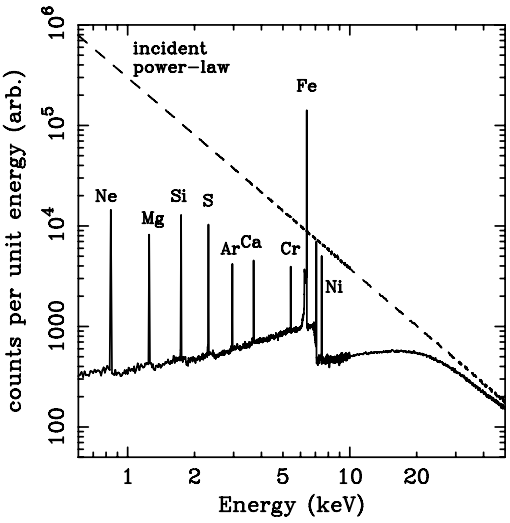

Fig. 1 Reflection from a cold neutral slab of matter with cosmic abundances, illuminated by a power-law of index $\Gamma = 2$ (Reynolds 1996)

2 Reflection Spectra

2.1 Cold Reflection

X-ray reflection in the back-scattering sense was first introduced into X-ray astronomy by Basko et al. (1974) in a study of the reflection and reprocessing expected from the normal companion star in a Galactic X-ray binary system, such as Her X-1. They show using analytical methods that the albedo depends on the competition between electron scattering and photoelectric absorption, the former dominating above 20 keV and the latter at lower energies. Compton recoil is increasingly important at higher energies which leads to a hump in the reflection spectrum at 20–40 keV, known as the Compton hump. Milgrom and Salpeter (1975), and Felsteiner and Opher (1976) tackled the same problem, the latter using a Monte-Carlo approach, which is time-consuming, but can give precise and straightforward results, particularly with regard to angular dependencies, for neutral material (Fig. 1). We used this approach to model X-ray reflection from the accretion column on a white dwarf (Swank et al. 1984).

Interest in X-ray reflection from the innermost regions around accreting black holes began with the work of Guilbert and Rees (1988) who argued that cold material should be common in that environment and so would create spectral features. This prompted Lightman and White (1988) to compute in detail the reflection continuum in a Green's function approach, which lends itself to rapid computation (XSPEC model PEXRAV; Magdziarz and Zdziarski 1995).

Note that this last approach does not include the fluorescent emission lines which are produced by de-excitation of atoms which have photoelectrically absorbed the X-rays. Hard X-rays are mostly absorbed by the ejection of a K-shell electron in iron or other abundant high atomic number, Z, element. The K-shell is then filled by an outer electron, the energy released either emerging as an Auger electron or K-shell fluorescent line. The fluorescent yield varies as Z^4, so line emission is particularly strong for iron (Fig. 1). Monte-Carlo computations of X-ray fluorescent emission were published by George and Fabian (1991) and Matt et al. (1991) giving line strength, angular dependencies etc. The equivalent width of the fluorescent iron line produced by irradiation of cosmic matter is about 150 eV.

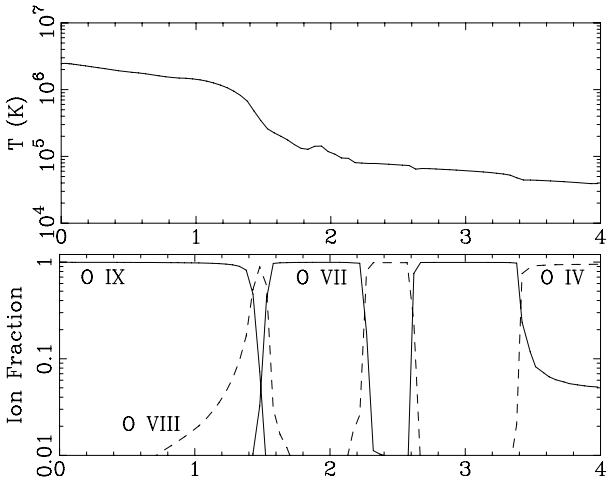

Fig. 2 Development of temperature and oxygen ionization fractions with Thomson depth (x-axis) into a slab illuminated by a power-law with $\Gamma = 2$ (Ross and Fabian 2005). The calculations are performed self-consistently with the Ross (1979) code

2.2 Ionized Reflection

The work described so far assumes that the irradiation is weak and the gas dense, so it remains neutral, which is unlikely in the inner region around a luminous accreting black hole or neutron star. It is expected that the irradiation is intense enough to ionize at least the surface of the flow. There might also be radiation intrinsic to the flow (e.g. thermal black body emission) which also ionizes the matter. In the first circumstance, the situation is non-linear and more detailed computations are required.

One of us (Ross 1979) had written a computer code for dealing with the transfer of X-rays through gas which is optically thick to Compton scattering. The code computes the spatial transport of the continuum radiation in the diffusion approximation and its energy redistribution through the Fokker-Planck approximation. The Cooper (1971) Fokker-Planck operator is now used to describe the effects of Compton scattering, since it correctly handles effects such as the reduction in scattering rate at high energies due to the reduction in the Klein-Nishina cross section for photon energies up to 1 MeV. The ionization and thermal balance are self-consistently computed in step with the development of the radiation field, leading to a layered ionization structure of an irradiated slab (Fig. 2).

The code was used to model the spectrum of accretion discs in Active Galactic Nuclei (AGN; Ross and Fabian 1993). At low ionization parameter ($\xi = 4\pi F/n$, where F is the incident flux and n is the number density of hydrogen nuclei) it reproduces the results of Lightman and White (1988), self-consistently with the fluorescent lines, and at higher ξ it shows the lower Z elements becoming ionized thereby softening the reflection spectrum. Conservation of energy means that the loss of albedo at high energy leads to a soft hump of emission at low energies, composed of lines and bremsstrahlung. At high ξ the surface of the slab is so highly ionized so that most lines originate at Thomson depths of several, scattering their way out, so becoming Compton and thermal broadened in the process.

Further developments in the code (e.g. Ross et al. 1999) have led to more elements and lines being considered culminating in a very extensive grid of models being available for XSPEC fitting (REFLIONX Ross and Fabian 2005; Fig. 3). This model captures the strongest lines and continuum behavior and should be robust and reliable for fitting CCD quality spectra, or if relativistic blurring is employed. A major advantage of the Ross code is its speed, which means that large grids (where, say, photon index Γ, abundance A, ξ and/or other parameters are varied) can be computed in a few weeks.

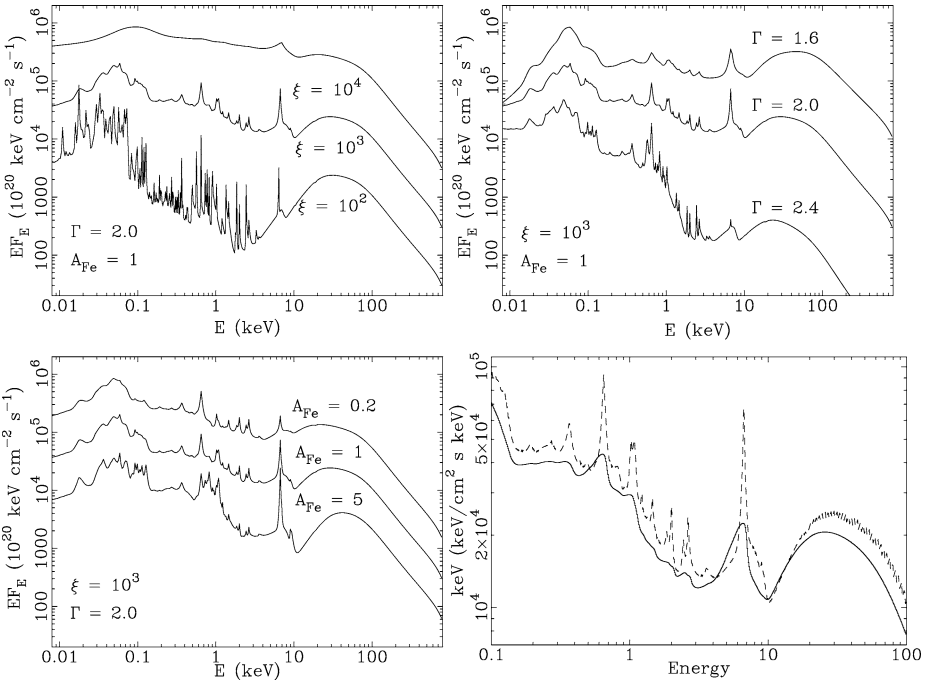

Fig. 3 Reflection from a constant-density slab at differing ionization parameters (ξ, *top left*), photon index (Γ, *top right*) and iron abundance ($A_{\rm Fe}$, *lower left*). A typical spectrum is shown at lower right before (*dashed*) and after (*solid*) relativistic blurring. From Ross and Fabian (2005)

The strength of the iron line as a function of ξ was studied by Matt et al. (1993, 1996). This shows that the line is depressed when $\xi \sim 100$–500 due to assumed Auger destruction. This occurs for photons produced by fluorescence of Fe XVII–XXII, which are resonantly trapped by the next more highly ionized species of iron, co-existing with the originating ion. There is a high probability of autoionization (Auger effect) at each scattering, so the line is rapidly destroyed (Ross et al. 1996). The extent to which this happens in practice depends, however, on how multiple the lines are, and turbulent the gas is (see Liedahl 2005 for further discussion).

The work has been extended to cover the conditions expected in discs around stellar mass black holes where thermal emission from within the disc can affect the ionization balance of oxygen and iron, for example. For the same value of irradiated ξ the material is more highly ionized and the lines broader (since the gas is hotter, thermal broadening is higher then for the AGN case, where the disc temperatures are much lower; see Fig. 5).

Several other codes, approaches and assumptions have been made. Zycki et al. (1994) used a Monte-Carlo method, treating photons in the 0.15–100 keV and ignoring the thermal emission from the gas itself. This led to higher surface temperatures and steeper temperature gradients than for the Ross code, resulting in differences below 0.3 keV. Dumont et al. (2003) use the Titan code which employs "accelerated lambda iteration" for the radiation transfer (see also Rózańska et al. 2002). This has the drawback that it is very time-consuming. Dumont et al strongly criticise the escape probability formalism used for the emission lines by Ross and Fabian yet, as shown by Ross and Fabian (2005), their results agree very well in detail. Further computations are presented by Rózańska and Madej (2008) using a sep-

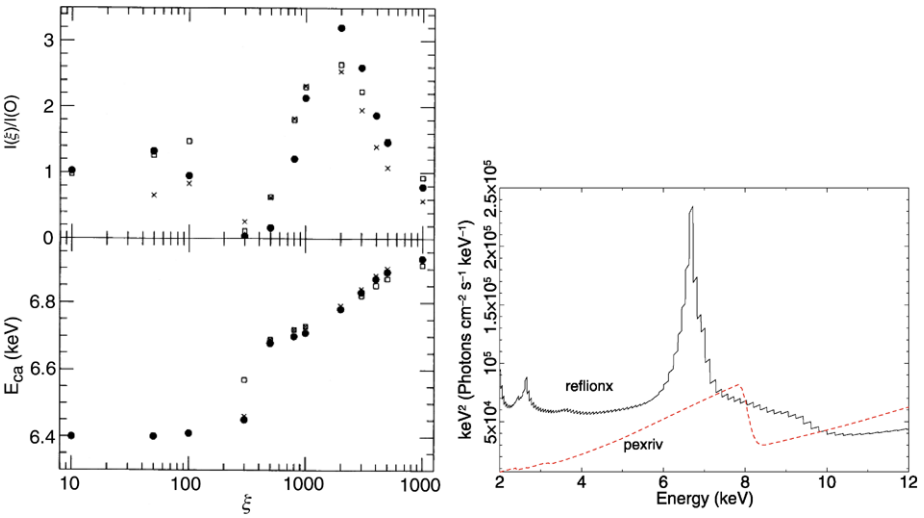

Fig. 4 Strength of total iron line (relative to that from neutral matter) versus ionization parameter (*upper left panel*, Matt et al. 1993). The dip in line strength at $\xi \sim 150$–500 is due to assumed auger destruction. The *lower left panel* gives the mean energy of the iron line. The *right panel* compares the result from REFLIONX (Ross and Fabian 2005) with PEXRIV (Magdziarz and Zdziarski 1995) when $\xi = 1000$

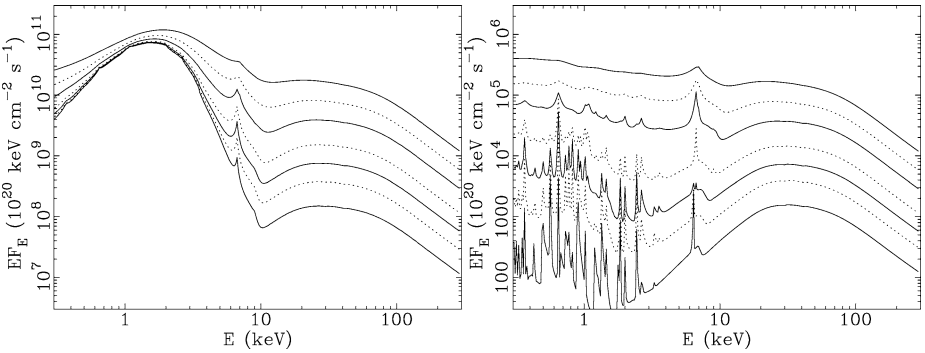

Fig. 5 Self-consistent ionized reflection calculations for an irradiated slab with (*left*; Ross and Fabian 2007) and without (*right*; Ross and Fabian 2005) internal heating. The first is appropriate for a Galactic Black Hole system and the second for an AGN

arate code. An interesting new set of computations, which have many line transitions and potentially cover a wide range of parameters, have been made at high spectral resolution by Garcia and Kallman (2010; Fig. 6), stemming from the well-known XSTAR photoionization code. Where the same parameters have been used, the results agree well with the Ross code.

In passing, we note attempts to make fast approximations for ionized disks (e.g. Done et al. 1992, PEXRIV; Magdziarz and Zdziarski 1995) following the basic Lightman and White (1988), Green's function approach. A comparison for $\xi = 1000$ between REFLIONX and PEXRIV is shown in Fig. 4. The continua are clearly very different (PEXRIV does not compute the emission line, which needs to be added). This is partly because PEXRIV does not the include the Compton blurring which occurs as the photons scatter out of the slab. We strongly advise against using PEXRIV to model highly ionized reflection. There are exam-

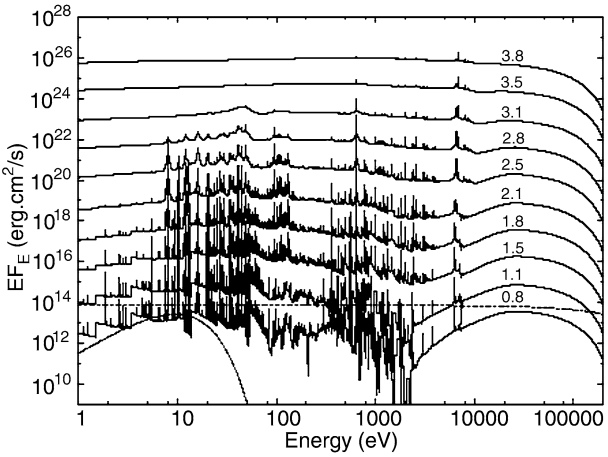

Fig. 6 Self-consistent reflection spectra from Garcia and Kallman (2010). These spectra have many more lines than those of Ross and Fabian (2005) but are in broad agreement when viewed at low resolution (or are relativistically blurred)

ples in the literature where the presence of ionized reflection has been ruled out erroneously using PEXRIV as the reflection model; the strong cusp it predicts around 7–8 keV being absent from the data.

Finally, we note that the iron K-edge in the reflection spectrum from ionized gas is smeared by Comptonization (Fig. 3), and may appear smeared further by relativistic motions close to the compact object. This can be modelled by the smeared edge model SMEDGE (Ebisawa 1992). We strongly caution against using this alone unless the cause of the smearing (strong Comptonization and/or relativistic blurring) are an implicit part of the underlying physical model. Again note that it should be accompanied by a similarly blurred iron emission line.

2.3 Hydrostatic Equilibrium or Not?

Nayakshin et al. (2000) rightly point out that the slabs discussed above would not be in *hydrostatic* equilibrium if they represent the surface of an accretion disc. They use a combination of radiation transfer for a Compton-thick medium with XSTAR for the ionization and thermal balance, ensuring at the same time that the slab is in hydrostatic balance. The results are similar to the fixed density case, but with the features diluted (see also Ballantyne et al. 2001).

It is not clear, however, that hydrostatic equilibrium is relevant to the photospheres of luminous discs which are expected to be dominated by magnetic pressure in their outer parts (Blaes et al. 2007).

3 Relativistic Blurring

Ionized reflection is expected to occur around accreting black holes and neutron stars due to irradiation of the accretion flow by the primary, power-law, X-ray continuum. The dense parts of the flow are not, however, expected to be static but will at least be rotating in the disc. This means that Doppler shifts and gravitational redshifts (Fig. 7 left) need to be applied to the reflection spectrum before comparing with observations (Fabian et al. 1989; Laor 1991). Observing emission and absorption features of known laboratory wavelength from a relativistic accretion disc means that the geometry and other properties of the disc can be

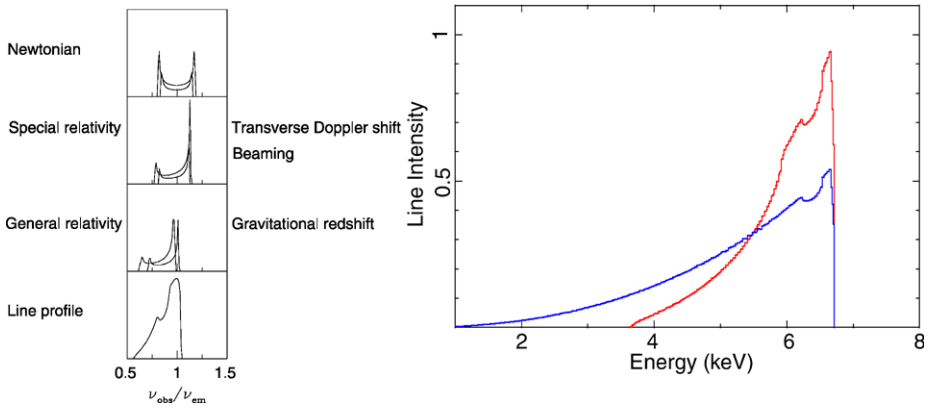

Fig. 7 The physics behind relativistic blurring around a black hole (*left*; Fabian et al. 2000). Comparison of line shapes from a disc around a non-spinning black hole (*black*) and a maximally-spinning one (*red*)

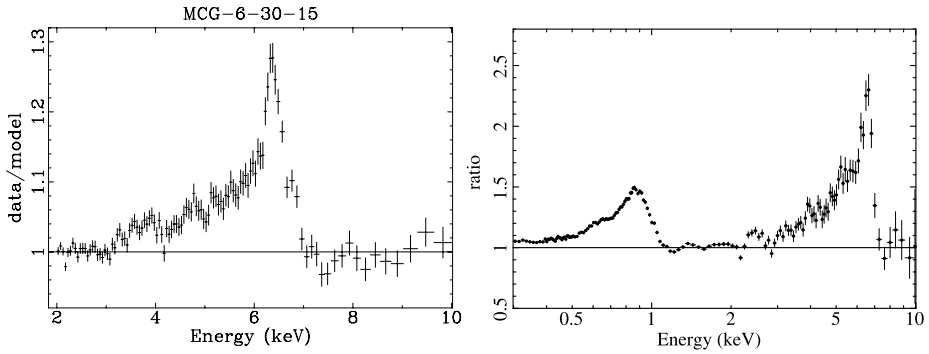

Fig. 8 The broad iron lines of the AGN MCG–6-30-15 (Fe-K, Fabian and Vaughan 2003) and 1H 0707-495 (Fe-L and K, Fabian et al. 2009). See Nandra et al. (2007) for more examples

determined. In particular the redward extent of an emission line is dependent on the strength of the gravitational redshift, which in turn depends on the innermost radius of the disc. Identifying that with the innermost stable circular orbit ISCO.[1] Bardeen et al. (1972) then enables the spin of the black hole to be measured (Fig. 7 right). Reviews of X-ray reflection in this context can be found in Fabian et al. (2000), Fabian and Miniutti (2005), Reynolds and Nowak (2003) and Miller et al. (2008).

The first clear signs of reflection from AGN emerged from GINGA data (Pounds et al. 1990; Matsuoka et al. 1990). The combination of a high cosmic abundance and high fluorescent yield make iron-K line emission stand out in the reflection spectrum. Relativistically-broadened iron lines were first found using ASCA data (Tanaka et al. 1995; Nandra et al. 1997) and are now routinely found from XMM-Newton and Suzaku spectra. The examples of MCG–6-30-15 and 1H 0707-495 are shown in Fig. 8, the latter also showing a strong broadened Fe-L line below 1 keV. These examples are clear because the iron

[1] See Reynolds and Fabian (2008) for discussion and calculations arguing that the ISCO is the appropriate radius in an ionized disc.

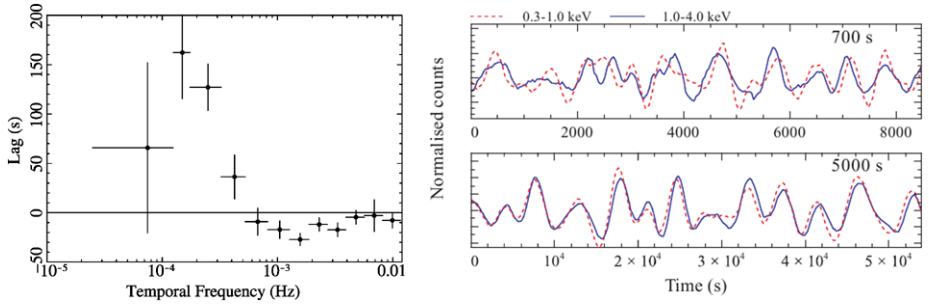

Fig. 9 The lags between the hard (1–4 keV) and soft (0.3–1 keV) flux in 1H 0707-495, showing that for rapid, high frequency variations the soft band, dominated by the Fe-L line (see Fig. 9) lags behind the power-law component which dominates the hard band. The *panel on the right* shows time-filtered light curves which show the lags (Zoghbi et al. 2010)

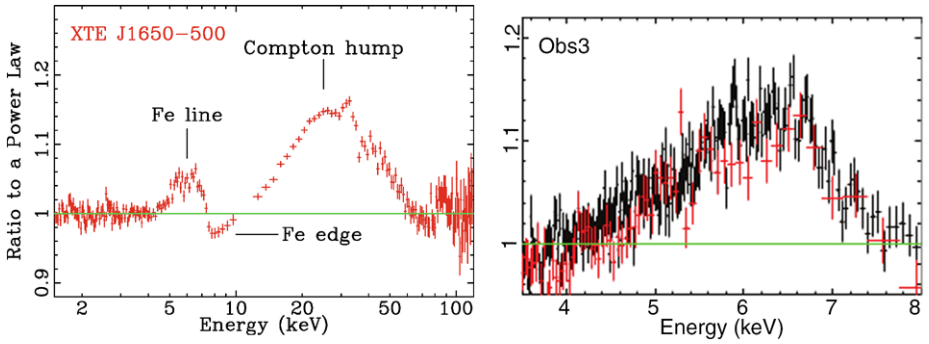

Fig. 10 Broad iron lines in a Galactic Black Hole binary system (Miniutti and Fabian 2004) and a neutron star system (Reis et al. 2009). See Miller et al. (2008) and Cackett et al. (2010) for more examples of black hole and neutron star systems respectively

abundance in the reflector is high, so enhancing the line strengths. The soft X-ray lines in the reflection spectrum at normal abundances tend to overlap each other so that they relativistically blur into a mildly-structured soft hump. This is identified as the soft excess seen in the spectra of many AGN (Crummy et al. 2006).

Alternative models for mimicking the spectrum have been made (see Fabian et al. 1995 for a discussion dismissing some of the models). Absorbers which partially cover the power-law source, so that photoelectric edges produce the sharp spectral features, can sometimes mimic these spectra, particularly if enough components are used and some generous systematic uncertainty is added to all data points (e.g. Miller et al. 2008). The geometry of such models is often unspecified, which raises issues in terms of the nature of clouds which only partially cover what is a highly compact source and how the timing properties are explained. The line emission which accompanies X-ray absorption is also often ignored.

The partial covering models often have all the activity occurring at 100 s to 1000 s r_g (100 s–1000 s gravitational radii). The best evidence that we are instead dealing with the innermost regions at a few r_g is found in the 30 s lag found in high frequency variations of the soft, iron-L line dominated band relative to the harder, power-law dominated band in 1H 0707-495 (Fig. 9; Fabian et al. 2009; Zoghbi et al. 2010). This is exactly what an

inner reflection model predicts, the lag being just the additional light travel time taken by the reflection signal compared to the direct power-law one; it is a reverberation or echo.

The strength of the reflection component relative to the power-law one depends not only on the geometry but also on the isotropy of the power-law source. Even an isotropic power-law source can appear anisotropic due to relativistic effects, either due to its motion through special relativity (Reynolds and Fabian 1997; Beloborodov 1999) or general relativistic light bending (Martocchia et al. 2000; Miniutti and Fabian 2004). Strong light bending (by radians) is indeed expected from emission regions close to a rapidly spinning black hole.

Broad iron lines are also common in the X-ray spectra of accreting stellar mass X-rays sources (Miller 2007 and accreting neutron stars (Cackett et al. 2010). Such systems are not in general obscured by rapidly-changing, partially-covering absorbing clouds, so such explanations cannot be relevant there. The lines shape and behaviour are however very similar to that seen in AGN, thereby demonstrating that relativistically-blurred reflection spectral components are an intrinsic property of accreting black holes.

Acknowledgements We thank our many collaborators, including T. Boller, D. Ballantyne, L. Brenneman, E. Cackett, L. Gallo, K. Iwasawa, J. Miller, G. Miniutti, K. Nandra, R. Reis, C. Reynolds, Y. Tanaka, P. Uttley, D. Walton, S. Vaughan, A. Young and A. Zoghbi.

References

D.R. Ballantyne, R.R. Ross, A.C. Fabian, Mon. Not. R. Astron. Soc. **327**, 10 (2001)
J.M. Bardeen, W.H. Press, S.A. Teukolsky, Astrophys. J. **178**, 347 (1972)
M.M. Basko, R.A. Sunyaev, L.G. Titarchuk, Astron. Astrophys. **31**, 249 (1974)
A.M. Beloborodov, Astrophys. J. **510**, L123 (1999)
O. Blaes, S. Hirose, J.H. Krolik, Astrophys. J. **664**, 1057 (2007)
E.M. Cackett et al., Astrophys. J. **720**, 205 (2010)
G. Cooper, Phys. Rev. D **3**, 2312 (1971)
J. Crummy, A.C. Fabian, L. Gallo, R.R. Ross, Mon. Not. R. Astron. Soc. **365**, 1067 (2006)
C. Done, J.S. Mulchaey, R.F. Mushotsky, K.A. Arnaud, Astrophys. J. **395**, 275 (1992)
A.-M. Dumont, S. Collin, F. Paletou, S. Coupé, O. Godet, D. Pelat, Astron. Astrophys. **407**, 13 (2003)
K. Ebisawa, PhD thesis, 1992
A.C. Fabian, M.J. Rees, L. Stella, N.E. White, Mon. Not. R. Astron. Soc. **238**, 729 (1989)
A.C. Fabian, K. Nandra, C.S. Reynolds, W.N. Brandt, C. Otani, Y. Tanaka, Mon. Not. R. Astron. Soc. **277**, L11 (1995)
A.C. Fabian, K. Iwasawa, C.S. Reynolds, A.J. Young, Publ. Astron. Soc. Pac. **1123**, 1145 (2000)
A.C. Fabian, S. Vaughan, Mon. Not. R. Astron. Soc. **340**, L28 (2003)
A.C. Fabian, G. Miniutti, astro-ph/0507409 (2005)
A.C. Fabian et al., Nature **459**, 540 (2009)
J. Felsteiner, R. Opher, Astron. Astrophys. **46**, 189 (1976)
J. Garcia, T.R. Kallman, Astrophys. J. **718**, 695 (2010)
I.M. George, A.C. Fabian, Mon. Not. R. Astron. Soc. **249**, 352 (1991)
P.W. Guilbert, M.J. Rees, Mon. Not. R. Astron. Soc. **233**, 475 (1988)
A. Laor, Astrophys. J. **376**, 90 (1991)
D. Liedahl, AIP Conf. **774**, 99 (2005)
A.P. Lightman, T.R. White, Astrophys. J. **335**, 57 (1988)
P. Magdziarz, A. Zdziarski, Mon. Not. R. Astron. Soc. **273** 837 (1995)
A. Martocchia, V. Karas, G. Matt, Mon. Not. R. Astron. Soc. **312**, 817 (2000)
M. Matsuoka, L. Piro, M. Yamauschi, T. Murakami, Astrophys. J. **361**, 440 (1990)
G. Matt, G.C. Perola, L. Piro, Astron. Astrophys. **247**, 25 (1991)
G. Matt, A.C. Fabian, R.R. Ross, Mon. Not. R. Astron. Soc. **262**, 179 (1993)
G. Matt, A.C. Fabian, R.R. Ross, Mon. Not. R. Astron. Soc. **278**, 1111 (1996)
M. Milgrom, E.E. Salpeter, Astrophys. J. **196**, 589 (1975)
L. Miller, T.J. Turner, J.N. Reeves, Astron. Astrophys. **483**, 437 (2008)
J. Miller, Annu. Rev. Astron. Astrophys. **45**, 441 (2007)
G. Miniutti, A.C. Fabian, Mon. Not. R. Astron. Soc. **349**, 1435 (2004)

K. Nandra, I.M. George, R.F. Mushotzky, T.J. Turner, T. Yaqoob, Astrophys. J. **477**, 602 (1997)
K. Nandra, P.M. O'Neill, I.M. George, J.N. Reeves, Mon. Not. R. Astron. Soc. **382**, 194 (2007)
S. Nayakshin, D. Kazanas, T.R. Kallman, Astrophys. J. **537**, 833 (2000)
K.A. Pounds, K. Nandra, G.C. Stewart, I.M. George, A.C. Fabian, Nature **344**, 132 (1990)
R.C. Reis, A.C. Fabian, A.J. Young, Mon. Not. R. Astron. Soc. **399**, 1 (2009)
C.S. Reynolds, PhD thesis, University of Cambridge, 1996
C.S. Reynolds, M.A. Nowak, Phys. Rev. **377**, 389 (2003)
C.S. Reynolds, A.C. Fabian, Mon. Not. R. Astron. Soc. **290**, 1 (1997)
C.S. Reynolds, A.C. Fabian, Astrophys. J. **675**, 1048 (2008)
R.R. Ross, Astrophys. J. **223**, 334 (1979)
R.R. Ross, A.C. Fabian, Mon. Not. R. Astron. Soc. **261**, 74 (1993)
R.R. Ross, A.C. Fabian, W.N. Brandt, Mon. Not. R. Astron. Soc. **278**, 1082 (1996)
R.R. Ross, A.C. Fabian, A.J. Young, Mon. Not. R. Astron. Soc. **306**, 461 (1999)
R.R. Ross, A.C. Fabian, Mon. Not. R. Astron. Soc. **358**, 211 (2005)
R.R. Ross, A.C. Fabian, Mon. Not. R. Astron. Soc. **381**, 1697 (2007)
A. Rózańska, A.-M. Dumont, B. Czerny, S. Bollin, Mon. Not. R. Astron. Soc. **332**, 799 (2002)
A. Rózańska, J. Madej, Mon. Not. R. Astron. Soc. **386**, 1872 (2008)
J.H. Swank, A.C. Fabian, R.R. Ross, Astrophys. J. **280**, 734 (1984)
Y. Tanaka et al., Nature **375**, 659 (1995)
A. Zoghbi et al., Mon. Not. R. Astron. Soc. **401**, 2419 (2010)
P.T. Zycki, J.H. Krolik, A.A. Zdziarski, T.R. Kallman, Astrophys. J. **437**, 597 (1994)